Dev Genes Evol (2002) 212:239–247
DOI 10.1007/s00427-002-0238-z

ORIGINAL ARTICLE

Jing Meng · Edwin C. Stephenson

Oocyte and embryonic cytoskeletal defects caused by mutations in the *Drosophila swallow* gene

Received: 14 December 2001 / Accepted: 19 March 2002 / Published online: 18 May 2002

Abstract The maternal effect gene *swallow* (*swa*) of *Drosophila* is required for *bicoid* and *htsN4* mRNA localization during oogenesis. *Swallow* is also required for additional, poorly understood, functions in early embryogenesis. We have examined the cytoskeleton in *swa* mutant oocytes and embryos by immunocytochemistry and confocal microscopy. Mid- and late-stage *swa* oocytes have defective cytoplasmic actin networks. Stage-10 oocytes have solid actin clumps and hollow actin spheres in the subcortical layer, and late-stage oocytes have uniformly distributed hollow actin spheres in the subcortical layer and in deeper cytoplasm. *Swa* preblastoderm embryos have uneven and irregularly distributed actin at the cortex, and defective subcortical actin networks that contain hollow and solid spheres. In *swa* syncytial blastoderm embryos, the abnormal actin cytoskeleton is associated with defects in nuclear distribution, migration and cleavage. Actin cytoskeletal defects correlate with spindle defects, suggesting that the abnormal organization of the actin cytoskeleton allows interaction of mitotic spindles, which induces defective nuclear divisions and loss of nuclei from the surface of the embryo.

Keywords *Drosophila* oogenesis · *bicoid* RNA · RNA localization · Cytoskeleton · Nuclear migration

Introduction

Messenger RNA localization plays an important role in determining cellular fate during development (Bashirullah et al. 1998), although in most cases the mechanism of the mRNA localization process is not well understood. The localization of *bicoid* mRNA at the anterior oocyte margin during *Drosophila* oogenesis is one of the most thoroughly studied examples. *Bicoid* mRNA is localized at the anterior oocyte margin, and the bicoid protein acts as an anterior morphogen in the early embryo. Three genes, *staufen*, *exuperantia* and *swallow*, are required for *bicoid* mRNA localization. Of these, the role of *staufen* is probably clearest: the stau protein is a member of a family of dsRNA-binding proteins (St Johnston et al. 1992) and probably associates directly with *bicoid* mRNA (Ferrandon et al. 1994, 1997). Exuperantia protein is also probably associated with a *bicoid* mRNA-containing particle (Wang and Hazelrigg 1994; Wilhelm et al. 2000).

The role of *swallow* in RNA localization is not as clear. There are no known homologs of swallow protein in any organism outside the genus *Drosophila*. A weak similarity to the RRM family of RNA-binding proteins (Chao et al. 1991) is probably not significant, as critical parts of the motif are absent from the *swallow* homolog of *D. pseudoobscura* (Huang et al. 2000). Swallow protein is restricted to the oocyte cortex, in a position consistent with its role in RNA localization (Schnorrer et al. 2000; Stephenson, in preparation). Several aspects of the *swa* embryonic phenotype have been interpreted as suggesting a role in cytoskeletal structure or regulation. The most prominent of the early embryonic defects are uneven nuclear migration to and/or retention at the embryonic margin in preblastoderm embryos, and asynchronous and defective mitotic divisions of syncytial blastoderm nuclei (Zalokar et al. 1975; Hegde and Stephenson 1993). Substantial but variable numbers of *swa* embryos die in early embryogenesis, well before organogenesis and differentiation. Of the embryos that survive to an incipient larval stage, all show defects in anterior development that result from the failure to localize *bicoid* mRNA and protein. Most such embryos also show defects in abdominal segmentation (Stephenson and Mahowald 1987; Meng and Stephenson, unpublished), a phenotype that may result either from the nuclear anomalies early in embryogenesis, or from the partial loss of posterior de-

Edited by C. Desplan

J. Meng · E.C. Stephenson (✉)
Department of Biological Sciences,
Coalition for Biomolecular Products,
University of Alabama, Tuscaloosa, AL 35487, USA
e-mail: estephen@bama.ua.edu
Tel.: +1-205-3481828, Fax: +1-205-3481786

terminant localization (Ferrandon et al. 1994; Pokrywka et al. 2000).

Since the loss of *bicoid* mRNA localization does not account for the early embryonic nuclear and abdominal segmentation defects (e.g. *exuperantia* embryos do not show comparable defects), these observations have been interpreted as suggesting additional roles for *swallow,* perhaps in regulating cytoskeletal organization. In support of this model, Zaccai and Lipshitz (1996) showed embryos from a *swa* mother with abnormal distributions of actin and spectrin. Two possible links between *swallow* function and cytoskeletal regulation are known. First, swa^{+} function is required for localization of *htsN4* mRNA, which encodes an adducin-like protein that probably functions in actin cytoskeletal regulation (Ding et al. 1993). Second, swa protein associates with DdlcI, the *Drosophila* homolog of the 8-kDa dynein light chain protein (Schnorrer et al. 2000), a component of the dynein and myosin V motor complexes.

In this paper, we have extended the characterization of cytoskeletal defects in oocytes and early embryos produced by *swa* mothers. We find that actin cytoskeletal defects are detectable in mid-oogenesis, the stage when swa^{+} function is first required for RNA localization. Defects in the actin cytoskeleton persist into early embryogenesis and are associated with defects in nuclear migration and cleavage. We believe these cytoskeletal defects account for the non-*bicoid*-related aspects of the *swa* mutant phenotype.

Materials and methods

Fly culture

Oregon R wild-type flies, $swa^{1497}/FM7$, $swa^{VA11}/FM7$, $swa^{384}/FM7$, and $swa^{TG31}/FM7$ flies were cultured on yeasted corn meal agar medium at 25°C. Transgenic flies expressing GFP-moesin (Edwards et al. 1997) under the control of the *spaghetti-squash* promoter were provided by Dr. Daniel Kiehart (Duke University).

Reagents

A mouse monoclonal anti-actin antibody was purchased from Chemicon International. Polyclonal rabbit anti-actin antibody, monoclonal mouse anti-α-tubulin antibody and TRITC-labeled phalloidin were purchased from Sigma. Rhodamine-labeled goat anti-rabbit, fluorescein-labeled goat anti-mouse, and rhodamine-labeled goat anti-mouse secondary antibodies were obtained from Chemicon. Taxol (Paclitaxel) was purchased from Sigma. Sytox Green was obtained from Molecular Probes. Mounting solution (Fluoromount-G) was obtained from Southern Biotechnology Associates. 37% formaldehyde was purchased from Fisher Scientific, and 10% ultrapure EM Grade formaldehyde was purchased from Polysciences.

Immunocytochemistry

Ovaries of Oregon R wild-type females and homozygous *swa* mutant females were dissected in PBS (Karr and Alberts 1986) and fixed in 5% formaldehyde in PBS for 20 min. After fixation, tissues were rinsed in several changes of 0.1% PBST (PBS plus 0.1% Triton X-100) for 30 min.

Embryos from Oregon R wild-type mothers and embryos from homozygous *swa* mutant mothers were collected on grape juice agar plates at 25°C. Embryos were brushed and rinsed from the plates with Triton/NaCl (0.05% Triton X-100, 0.7% NaCl, pH 7.4), and dechorionated in Chlorox:Triton/NaCl (1:1) for 3 min. Dechorionated embryos were rinsed with Triton/NaCl, and fixed by a modified procedure of Karr and Alberts (1986). Half a millilitre PEM buffer (0.1 M Pipes, 1 mM $MgCl_2$ and 1 mM EDTA, pH 6.9 adjusted with KOH) and 10 µl 5 µM Taxol in dimethylsulfoxide were added to the tube. After 1 min, the liquid was removed, 0.5 ml octane was added, the tube swirled gently and 0.5 ml 37% formaldehyde was added. The embryos were fixed for about 3 min. The formaldehyde phase was removed, 0.5 ml methanol was added, and the tube shaken vigorously to break the vitelline membrane. The de-vitellinized embryos were post-fixed in pure methanol for about 15 min. The embryos were re-hydrated by 5-min washes in 3:1, 1:1, 1:3 methanol:0.01% PBST and in pure 0.01% PBST (PBS plus 0.01% Triton X-100). Embryos to be stained with Sytox Green were treated with RNaseA (50 µg/ml heat-treated RNaseA in 0.01% PBST; 30 min at 37°C). Embryos were washed in four changes of 0.01% PBST.

For oocyte actin staining, fixed egg chambers were incubated in 0.1 µg/µl TRITC-labeled phalloidin in 0.1% PBST for 4 h at room temperature, and washed in 0.1% PBST for 1 h with several changes. The tissues were mounted in Fluoromount-G.

For actin and nuclear double staining, the embryos were incubated in a 1:100 dilution of anti-actin antibody in 0.01% PBST overnight at 4°C. For tubulin and nuclear double staining, the embryos were incubated in a 1:500 dilution of monoclonal anti-tubulin antibody overnight at 4°C. After overnight incubation, embryos were washed in several changes of 0.01% PBST for 1.5 h. Then the embryos were incubated in 1:500 diluted secondary antibody in 0.01% PBST for 1 h at 25°C, and washed in TBS (0.8% NaCl, 0.02% KCl, 0.3% Tris-HCI, pH 7.4) for 2 h with several changes. These embryos were then stained in 0.5 µM Sytox Green for 50 min and washed in four changes of TBS.

For actin and tubulin double staining, the embryos were first treated with 1% BST (PBST containing 1% BSA) for 3–5 h. They were then incubated with the two primary antibodies at the dilutions described above, overnight at 4°C, washed in PBST for 2 h with several changes, and stained with both secondary antibodies at the dilutions above for 1 h. The embryos were washed in 0.01% PBST for 2 h with several changes, and mounted.

Observation of actin in living embryos

Wild-type embryos were from transgenic flies carrying a GFP-moesin transgene. *Swa* mutant embryos were from homozygous swa^{VA11} mutant mothers carrying a GFP-moesin transgene. Embryos were collected on grape juice plates for 90 min at 25°C, and removed from the plate onto moist filter paper. These embryos were rolled on the filter paper to remove sugar from the surface of the embryos, and transferred to a dry piece of filter paper. The embryos were transferred to a long coverslip, covered with a drop of halocarbon oil, and observed on an inverted laser-scanning confocal microscope. Embryos survived in this manner for at least 3 h.

Results

Actin cytoskeletal defects in mid- and late-stage swa mutant oocytes

To examine actin cytoskeletal organization in oocytes, we performed direct TRITC-phalloidin staining for actin. We found improved labeling of internal actin structures with the longer than customary phalloidin incubation times used here. We examined the actin cytoskeleton in

over 500 egg chambers from homozygous *swa* females and over 200 wild-type egg chambers.

In wild-type mid-stage oocytes, most actin is uniformly and evenly distributed at the cortical surface. Beneath the cortical layer, deeper actin networks are also uniform, but much less concentrated (Fig. 1A). In late oocytes, the uniform subcortical actin network is filled with uniformly distributed fine fibers, tiny actin granules and many holes which lack actin. These holes presumably are yolk granules and lipid droplets (Fig. 1B, C).

Defects in actin organization are first detectable at about stage 10 in oocytes from strong mutants, such as swa^{VA11}, swa^{1497}, and swa^{384}. The following results are pooled observations on oocytes from these three alleles, which are equivalent in phenotype. Small irregularly-shaped actin aggregates and actin spheres are observed below the actin-rich cortical layer (Fig. 1D). Serial sections (not shown) establish that most of the actin spheres are "hollow," that is have an actin-rich surface and an actin-poor core. About 30% of stage-10 oocytes show a relatively mild abnormal phenotype in which only a few clumps and spheres are present and are limited to the anterior subcortical layer of the oocyte. About 10% of stage-10 egg chambers show a larger number of aggregates and spheres, which are distributed throughout the oocyte, and fused actin spheres (arrow in Fig. 1D).

Similar defects are observed in later oocytes from the three strong alleles. About 60% of oocytes between stages 11 and 14 have detectable defects in actin organization. In these abnormal oocytes, actin spheres of about 3–5 μm in diameter are uniformly distributed from the subcortical layer into deeper central cytoplasm (Fig. 1E, F). The spheres are more numerous in later stages of oogenesis, and a larger fraction of them are hollow. Occasional "double" spheres consist of two spheres fused at their surface (arrow in Fig. 1E). Tiny actin granules are usually visible on the surface of the spheres. The cores of the spheres have variable amounts of actin, but most spheres in late oocytes are hollow.

These defective actin structures were observed in oocytes from the strong *swa* alleles *1497*, *384* and *VA11* but not in the weak allele *TG31*. There is no significant difference among the strong alleles in frequency and severity of the defective structures. Moreover, in living swa^{VA11} egg chambers expressing a GFP-moesin construct, we observed the same defects in actin distribution (not shown). The cortical microtubule cytoskeleton in *swa* mutant oocytes does not show comparable defects (not shown).

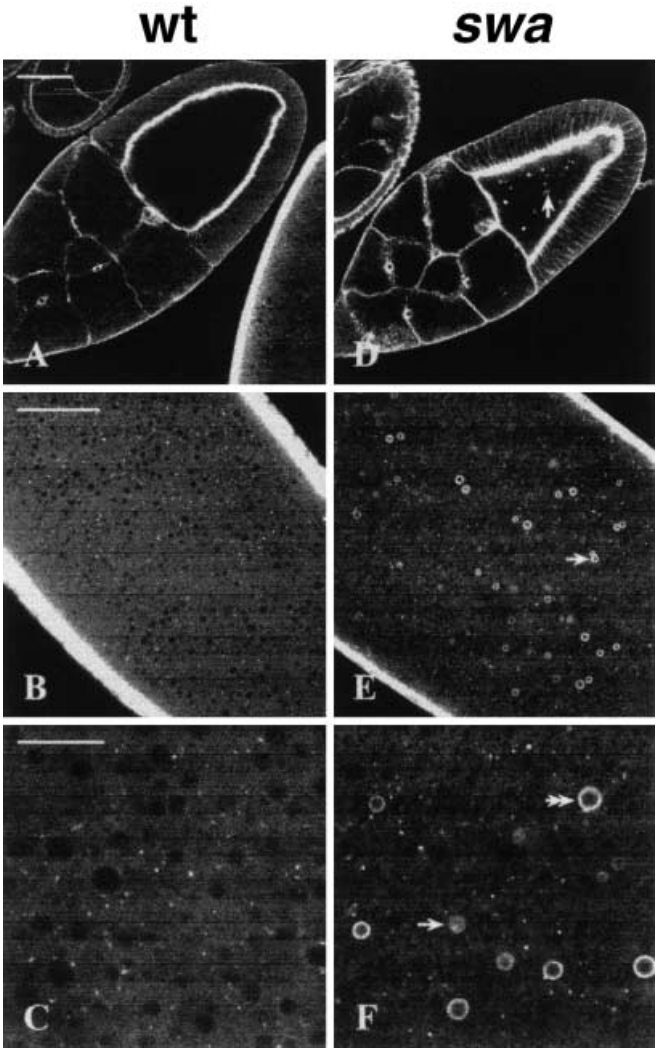

Fig. 1A–F Actin cytoskeletal defects in oocytes. Confocal images of wild-type and *swallow* egg chambers. Rhodamine-phalloidin staining. The *bar* in **A** is 50 μm and applies to **A** and **D**; the *bar* in **B** is 50 μm and applies to **B** and **E**; the bar in **C** is 20 μm and applies to **C** and **F**. **A** Wild-type stage-10 egg chamber. Medial optical section. **B** Wild-type stage-12 oocyte. Note the uniform subcortical actin network. **C** Wild-type stage-12 oocyte. Higher magnification of the subcortical actin network, consisting of variable sized holes that lack actin, and tiny actin-rich granules. **D** *Swa* mutant stage-10 egg chamber. Note the defective subcortical actin network of the oocyte, containing actin clumps and hollow spheres. Some of the actin spheres are fused (*arrow*). **E** *Swa* mutant stage-12 oocyte. Defective subcortical actin network, containing uniformly distributed hollow actin spheres (about 3–5 μm in diameter), small actin granules and actin-poor "holes." *Arrow* points to two hollow spheres fused at their surface. **F** *Swa* mutant stage-12 oocyte. Higher magnification of the defective subcortical actin network. The *arrow* indicates a grazing section through one sphere, and the *double arrow* shows a medial section through another sphere

Actin cytoskeletal defects in preblastoderm swa embryos

Embryogenesis in *Drosophila* begins with 13 syncytial mitotic divisions. The reorganization of the cytoskeleton plays a critical role at these stages. Nuclei of cycle 1 to cycle 3 embryos are restricted to the anterior half of the embryo in a spherical shape. In cycle 4 to cycle 6, nuclei migrate toward the posterior, a process known as axial expansion, and form an ellipsoid shape inside the embryo. The axial expansion movement depends on an intact actin cytoskeleton (Hatanaka and Okada 1991; von

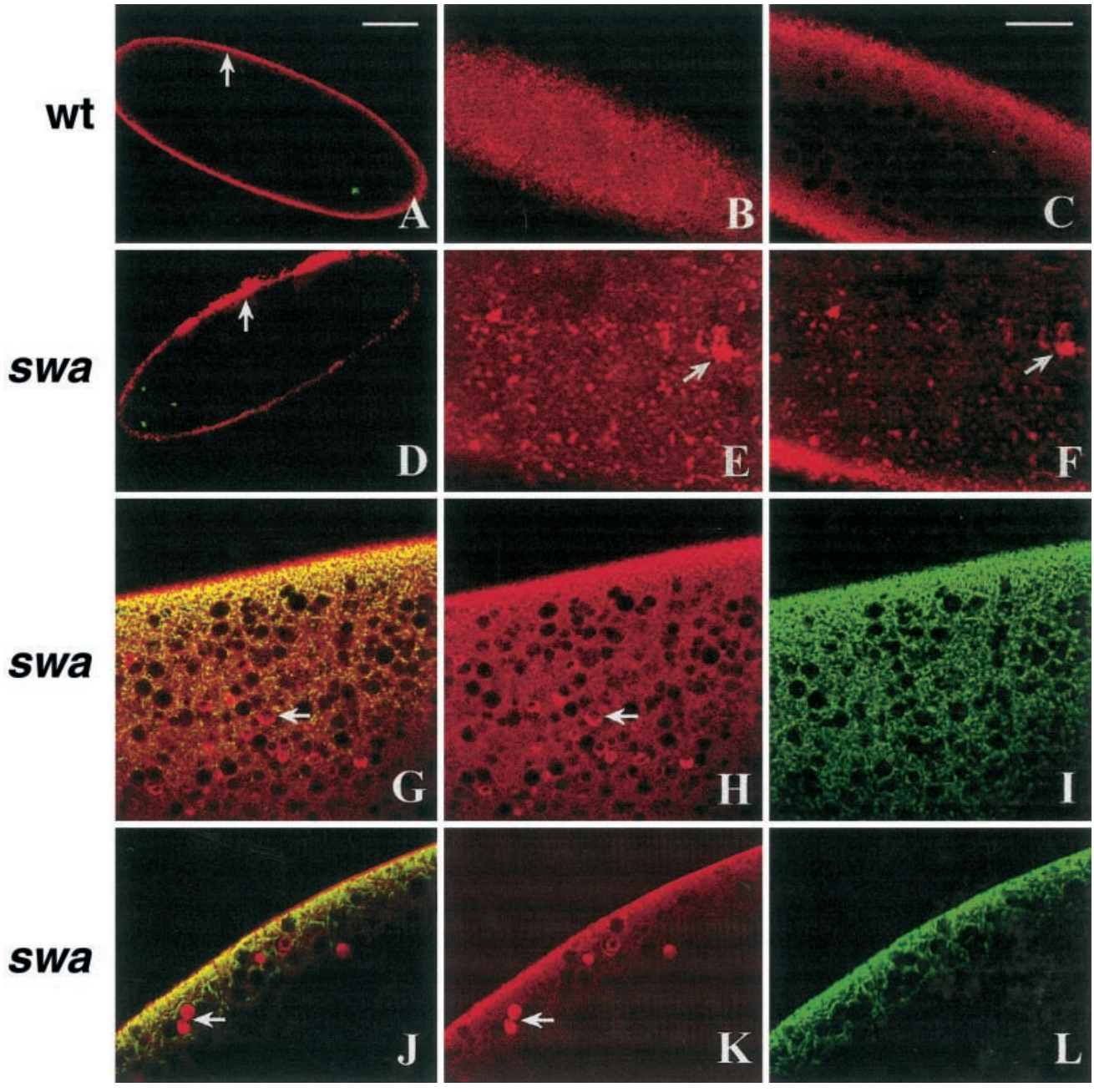

Fig. 2A–L Actin cytoskeletal defects in early *swa* embryos. Confocal images of wild-type and *swa* preblastoderm embryos. In **A**–**F**, actin is *red* and DNA is *green*; in **G**–**L**, actin is *red* and tubulin is *green*. The *bar* in **A** is 50 µm and applies to **A** and **D**; the *bar* in **C** is 20 µm and applies to the remaining panels. **A** Wild-type cycle-1 embryo. Medial optical section. The actin cortex is continuous and uniform (*arrow*). **B** Wild-type cycle-1 embryo. Grazing section, uniform and punctate actin cortex. **C** Wild type. Same embryo as in **B**, but 4 µm deeper. Less dense subcortical actin network is continuous except for spheres that lack actin. **D** *Swa* embryo, approximately cycle 2. The cortical actin layer is non-uniform in thickness and concentration (*arrow*). **E** *Swa* embryo, approximately cycle 1. Higher magnification of a grazing section through the surface of a *swa* embryo. Irregular actin aggregates are present at the cortex (*arrow*). **F** *Swa* embryo. A deeper section of the same embryo as in **E**. Actin clumps are also present in the subcortical layer (*arrow*). **G**–**I** *Swa* embryo, approximately cycle1. **G** is the composite of **H** and **I**. Actin spheres are present in the subcortical cytoplasm. Some spheres have walls of uneven thickness (*arrow* in **G** and **H**). In contrast to actin, tubulin distribution is uniform and even (**I**). **J**–**L** *Swa* embryo, approximately cycle 1. Medial section. **J** is the composite of **K** and **L**. Solid and fused actin spheres are present in the cytoplasm (*arrow* in **J** and **K**). In contrast to actin, tubulin distribution is normal (**L**)

Dassow and Schubiger 1994). From cycle 7 to cycle 9, nuclei migrate toward the embryonic periphery through an interaction between the microtubules of migrating nuclei and the yolk nuclei (Baker et al. 1993).

To examine actin cytoskeletal organization in early embryos, we performed indirect double immunofluorescent staining for actin and DNA on wild-type and *swa* preblastoderm embryos. DNA staining allowed us to de-

termine the number of nuclei in the embryo, and thus the approximate developmental stage of each embryo. We also performed actin and tubulin double staining on wild-type and *swa* early embryos.

In wild-type early embryos a dense and uniform actin layer lies just beneath the surface (Fig. 2B). This cortical layer is approximately 3 µm in thickness, and is uniform and continuous (Fig. 2A). Beneath the cortical actin layer is a much less dense subcortical actin network (Fig. 2C), which is continuous except for spherical holes that lack actin, presumably yolk granules and lipid droplets.

The actin defects we observed in *swa* oocytes persist into *swa* preblastoderm embryos. In embryos produced by *swa* mothers, the actin cortex has variable thickness and concentration, and actin distribution is uneven (Fig. 2D). Sometimes this unevenness takes the form of large aggregates of concentrated actin (arrow in Fig. 2D), while other parts of the cortex have little or no actin. Actin aggregates of various sizes are present in the cortical and subcortical regions (Fig. 2E, F), and *swa* embryos showing abnormal actin cortex have defective subcortical networks (Fig. 2E, F are from one *swa* mutant embryo). In most cases, the fine and uniform actin meshwork is replaced by many small actin aggregates (Fig. 2F) and spheres (Fig. 2G, J). Actin spheres in embryos are about 3–6 µm in diameter, slightly larger than those in oocytes. In contrast to the fairly uniform hollow spheres in oocytes, many actin spheres in early embryos have walls of non-uniform thickness (arrow in Fig. 2G, H), and some are solid (arrow in Fig. 2J, K). Of approximately 100 cycle-1 embryos observed in this study, about 50% show actin abnormalities. However we have never observed any anomalies in tubulin distribution (Fig. 2G–L).

Actin cytoskeletal defects in swa syncytial blastoderm embryos

In wild-type embryos, nuclei migrate to the surface by cycle 9 and then undergo four syncytial blastoderm mitoses. These nuclei form a monolayer at the periphery. The succeeding mitoses in syncytial blastoderm embryos require the reorganization of the actin and microtubule cytoskeletons (reviewed in Sullivan and Theurkauf 1995). During interphase, actin fibers are clustered as caps over each nucleus, and microtubules are organized as asters above each nucleus. During prophase, microtubules are reorganized into the spindle, and the actin cytoskeleton reorganizes as mitotic furrows that separate adjacent spindles in discrete compartments (Fig. 3A).

We have examined the organization of the actin cytoskeleton in *swa* mutant syncytial blastoderm embryos. The most common defects at this stage are non-uniformity in the depth of furrows (Fig. 3B, C) and incomplete actin compartments that enclose two closely spaced nuclei (arrows in Fig. 3C, D). Other actin compartments

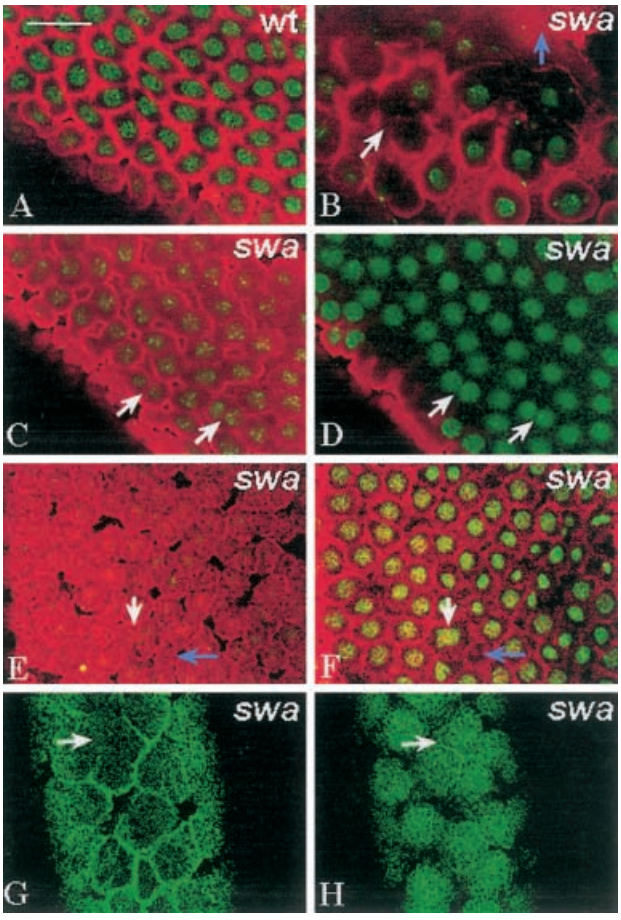

Fig. 3A–H Abnormal actin cytoskeleton in *swa* syncytial blastoderm embryos. Confocal images of wild-type and *swa* syncytial blastoderm embryos. In **A**–**F**, actin is *red* and DNA is *green*; in **G** and **H**, actin staining revealed by GFP-moesin localization is *green*. The *bar* in **A** is 20 µm and applies to all panels. **A** Wild-type cycle-12 syncytial blastoderm embryo. Actin furrows and nuclei form a regular honeycomb pattern. **B** *Swa* syncytial blastoderm embryo, approximately cycle 11 (the stage is an estimate since uneven nuclear distribution and asynchronous nuclear migration often make assignment uncertain). The *white arrow* points to the fusion of three actin furrow compartments, surrounding only one nucleus. The *blue arrow* indicates one actin clump, without nearby nuclei. **C** *Swa* syncytial blastoderm embryo, approximately cycle 12. *Each arrow* shows an incomplete actin furrow compartment surrounding two nuclei. **D** The same *swa* embryo as in **C**, but at a focal plane 9 µm deeper. The *arrows* show closely spaced nuclei due to the incomplete actin furrows. **E** *Swa* syncytial blastoderm embryo, approximately cycle 13. The *white arrow* indicates one defective and oversized actin compartment. The *blue arrow* shows one undersized actin compartment. **F** The same *swa* embryos as in E, at a focal plane 3 µm deeper**.** The *white arrow* indicates a polyploid nucleus surrounded by an oversized incomplete actin compartment. The *blue arrow* shows that the undersized actin compartment lacks a nucleus. **G, H** *swa* syncytial blastoderm embryo, anaphase (**G**) and the subsequent interphase (**H**) of cycle 12. Actin-containing structures in living embryos visualized by a moesin-GFP fusion protein. A large compartment with incomplete pseudocleavage furrows (*arrow* in **G**) resolves into a cluster of fused actin caps at the subsequent interphase (*arrow* in **H**)

lack nuclei (white arrow in Fig. 3B). Oversized actin compartments are visible, and these frequently contain large, heavily staining, probably polyploid nuclei (white arrow in Fig. 3E, F). Undersized compartments that lack nuclei are also observed (blue arrow in Fig. 3E, F). To examine the dynamics of actin organization, we followed blastoderm syncytial cleavages in living embryos from wild-type and *swa* transgenic flies expressing GFP-moesin. Incomplete or defective actin furrows at metaphase and anaphase (arrow in Fig. 3G) result in fused actin caps at interphase of the subsequent cell cycle (arrow in Fig. 3H).

Nuclear migration and cleavage defects in swa syncytial blastoderm embryos

Embryos produced by wild-type and *swa* mutant females were stained with an anti-tubulin antibody and Sytox Green, or with an anti-actin antibody and Sytox Green, and nuclear behavior was observed. In wild-type embryos, nuclei migrate to the surface of the embryo synchronously by cycle 9, and form a uniform nuclear monolayer during the blastoderm stage (Fig. 4A). Dividing nuclei in wild-type syncytial blastoderm embryos are evenly spaced (Fig. 4B).

Swa syncytial embryos have numerous defects in nuclear and mitotic behavior:

1. Nuclei migrate prematurely and asynchronously to the surface (Fig. 4C, E). Some nuclei are present in the subcortical layer at a stage when other nuclei have reached the periphery (Fig. 4C). We do not know whether these subcortical nuclei are late in migrating to the surface or reached the surface earlier and have sunk into the interior of the embryo. In some *swa* mutant embryos, some nuclei arrive at the periphery of the embryo before cycle 8. The white arrow in Fig. 4E points to a nucleus which has arrived at the cortex at about cycle 4.
2. Fusion of adjacent spindles (Fig. 4D).
3. Microtubule asters without associated nuclei in preblastoderm (Fig. 4E) and syncytial blastoderm embryos (Fig. 4F, H).
4. Tripolar spindles (Fig. 4I).
5. Polyploid nuclei in preblastoderm embryos (Fig. 4E, blue arrow) and blastoderm embryos (Fig. 3F, white arrow).
6. Uneven distribution of nuclei in syncytial blastoderm embryos (Fig. 4F–H). In Fig. 4H, the nuclear density of the central region of the embryo (outlined by the blue bar) is higher than that of the anterior and posterior parts of the embryo.
7. Asynchrony in the cell cycle (Fig. 4F–H). Nuclei in interphase, metaphase, anaphase and telophase are often detected at the same time at the surface of the *swa* syncytial embryo.

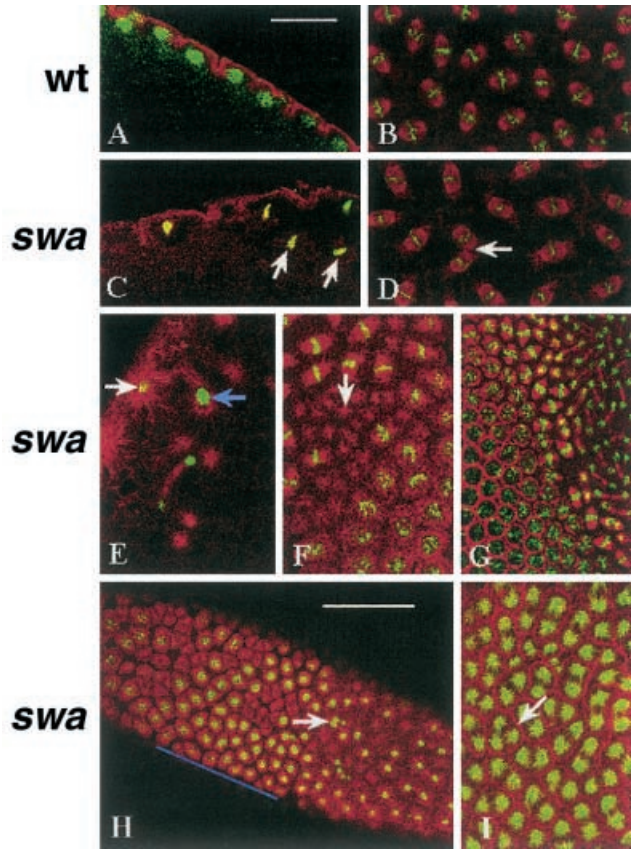

Fig. 4A–I Nuclear and cytoskeletal defects in *swa* syncytial embryos. Confocal images of wild-type and *swa* syncytial blastoderm embryos. In **A** and **C**, actin is *red* and DNA is *green*; in **B** and **D**–**H**, tubulin is *red* and DNA is *green*; in **I**, actin is *red* and tubulin is *green*. The *bar* in **A** is 20 µm and applies to all panels except **H**; the *bar* in **H** is 50 µm. **A** Wild-type cycle-12 syncytial blastoderm embryo. Nuclei migrate synchronously to the surface of the embryo, forming a uniform nuclear monolayer during the blastoderm stage. **B** Wild-type cycle-12 syncytial blastoderm embryo. Evenly spaced metaphase spindles. **C** *Swa* syncytial blastoderm embryo, approximately cycle 11. Subcortical nuclei are common (*arrows*), caused by asynchronous nuclear migration to the surface, or loss of defective nuclei from the surface. **D** *Swa* syncytial blastoderm embryo, approximately cycle 11. The *arrow* points to two fused mitotic spindles. **E** *Swa* syncytial blastoderm embryo, approximately cycle 4. Nuclei have reached the surface of the embryos prematurely. A few microtubule asters are not associated with nuclei. The astral fibers associated with one polyploid internal nucleus (*blue arrow*) interconnect with that of a nucleus (*white arrow*) which has already arrived at the cortex. **F** *Swa* syncytial blastoderm embryo, approximately cycle 12. A group of microtubule asters without associated nuclei is present (*arrow*). Nuclei at metaphase and prophase are both present. **G** *Swa* syncytial blastoderm embryo, approximately cycle 13. Loss of cell cycle synchrony. Nuclei in interphase, metaphase, telophase and anaphase are present. **H** *Swa* syncytial blastoderm embryo, approximately cycle 12. Several groups of microtubule asters without associated nuclei are present. The nuclei in the central part of the embryo *outlined with a blue bar* are one cycle ahead of those in the anterior and posterior parts of the embryo. The *arrow* points to two closely spaced nuclei that are probably about to fuse. **I** *Swa* syncytial blastoderm embryo, approximately cycle 12. The *arrow* points to a tripolar spindle

Discussion

The subcellular localization of mRNA molecules is a widespread mechanism for establishing developmental pattern (Bashirullah et al. 1998). In *Drosophila*, *bicoid* mRNA is localized to the anterior margin of stage 10–14 oocytes, and the resulting gradient of bicoid protein determines anterior-posterior embryonic pattern (Berleth et al. 1988; Driever and Nüsslein-Volhard 1988). *Swallow*$^{+}$ function is required for *bicoid* mRNA localization, and all embryos produced by *swa*/*swa* homozygous mothers that develop to late embryogenesis have anterior defects that result from the failure to localize *bicoid* mRNA. Many early embryos also show nuclear cleavage defects and arrest early in embryogenesis, and the embryos that survive to an incipient larval stage often have abdominal segmentation defects (Zalokar et al. 1975; Frohnhöfer and Nüsslein-Volhard 1987; Hegde and Stephenson 1993; Meng and Stephenson, unpublished). These latter phenotypes are difficult to reconcile with a simple failure to localize *bicoid* mRNA and have been interpreted as reflecting a role for *swa* in cytoskeletal regulation.

In this work we expand on an earlier observation of Zaccai and Lipshitz (1996) who found abnormal organization of actin and spectrin in early *swa* embryos. We show here that these actin defects originate in mid-oogenesis. With respect to the organization of the actin cytoskeleton, our primary conclusions are the following. (1) Abnormalities in actin cytoskeletal organization are first detectable in vitellogenic stage oocytes as small actin aggregates and spherical actin-containing structures in the oocyte subcortex. These aggregates and spheres persist throughout oogenesis and increase in number and distribution. (2) *Swallow* preblastoderm embryos have uneven and irregularly distributed cortical actin and defective subcortical actin networks in addition to actin aggregates and spheres in subcortical cytoplasm. (3) During the syncytial blastoderm stage some actin pseudocleavage furrows are either too shallow or absent altogether.

The actin cytoskeleton of *swa* oocytes is remarkable in two respects: there are substantial accumulations of internal filamentous actin, and most of these internal actin-containing structures have a curious morphology. The accumulation of non-cortical filamentous actin is abnormal since equivalent concentrations of filamentous actin are normally limited to the oocyte cortex (Theurkauf et al. 1992). To the best of our knowledge, structures similar to the actin spheres have not been previously reported. We are not certain of the origin of the amorphous actin aggregates in early embryos. The actin cytoskeleton is extensively reorganized at egg maturation (Theurkauf et al. 1992), so it is possible that some of the actin spheres are transformed at this time into the amorphous embryonic aggregates.

While actin defects are detectable in oogenesis, defects in microtubule distribution and organization have not been detected prior to early embryogenesis. Therefore, we conclude that defects in microtubule organization in *Drosophila* embryos are secondary to the actin defects, and are probably induced by earlier defects in actin organization.

We believe the defects in oocyte and embryonic actin organization account for the observed nuclear anomalies in early *swa* embryos. We find that nuclei migrate asynchronously and prematurely to the embryonic surface. While we cannot suggest a mechanistic explanation for this observation, we note that the axial expansion of preblastoderm nuclei requires actin filament function (Hatanaka and Okada 1991; von Dassow and Schubiger 1994). In *swa* syncytial blastoderm embryos, mitotic spindles sometimes fuse, presumably resulting in defective chromosomal segregation. Many nuclei are lost from the surface and sink into the center of the embryo (Hegde and Stephenson 1993). Large regions of the embryo are under-populated with nuclei, either because nuclei have never migrated to these regions, or because nuclei have not been retained at the periphery. These nuclear-free zones contain undersized actin-bound compartments and astral microtubules that are presumably organized by free centrosomes (Raff and Glover 1988; Yasuda et al. 1991). These observations are similar to the phenotypes of other mutants that affect actin organization (Sullivan et al. 1990, 1993; Postner et al. 1992), and to the phenotype of embryos injected with an anti-myosin antibody (Mermall and Miller 1995).

Our data support the model of Ding et al. (1993), who suggested that the syndrome of cytoskeletal and nuclear division defects in *swallow* mutant embryos results from the mislocalization of *htsN4* mRNA and protein. The presence of ectopic, internal htsN4 protein presumably nucleates the assembly of actin-spectrin complexes in internal non-cortical regions of the oocyte and embryo, where these structures should not exist. As an alternative, or in addition, reduced levels of cortical htsN4 protein may disrupt the cortical actin-spectrin cytoskeleton. In this work we show that the onset of detectable anomalies in actin organization occurs at oogenesis stage 10, the same stage as *htsN4* mRNA and protein mislocalization (Ding et al. 1993; Pokrywka et al. 2000; Zaccai and Lipshitz 1996). We observe anomalous internal actin structures first in the anterior oocyte, where concentrations of mislocalized *htsN4* mRNA and protein are highest. Defects in the actin cytoskeleton appear to be primary, since obvious defects in microtubule organization are not detectable until the syncytial blastoderm stage. At the blastoderm stage defects in nuclear behavior and division can be attributed to abnormalities in the actin cytoskeleton or to secondary consequences of earlier actin defects.

This model depends on the unproven assumption that the htsN4 adducin-like protein regulates actin-spectrin dynamics. Adducin probably acts to promote the assembly of the actin-spectrin membrane cytoskeleton (Gardner and Bennett 1987; Hughes and Bennett 1995; Kuhlman et al. 1996). However, the adducin-like proteins encoded by the *Drosophila hts* locus are apparently unique and their functions are not known. During *Drosophila* early

oogenesis, several adducin-like variants are components of the fusome, ring canals, and the oocyte cortex (Yue and Spradling 1992; Lin et al. 1994; Zaccai and Lipshitz 1996). Based on the partial structural similarity to adducin and their localization in cytoskeletal-rich structures, it is likely that adducin-like proteins also act in actin-spectrin regulation. However it is relevant to note that htsN4 and the other *Drosophila* adducin-like proteins lack the calmodulin-binding domain and kinase C phosphorylation site that are essential for all known adducin-actin interactions (Li et al. 1998; Matsuoka et al. 1998; Whittaker et al. 1999). Finally, the significance of the anterior localization of *htsN4* mRNA is also uncertain. It is reasonable that a cytoskeletal regulatory function like that envisioned for adducin-like proteins should be restricted to the oocyte cortex (where the actin-spectrin cytoskeleton is), but the significance of its localization to the anterior cortex is not obvious.

Direct tests of the model that the cytoskeletal effects of *swallow* mutants are mediated entirely through htsN4 mislocalization are possible, though not simple. The model predicts that the severity of the *swallow* cytoskeletal and nuclear phenotype should be affected by mutations at the *hts* locus. This experiment is complex in interpretation because we do not know whether the presence of internal htsN4 protein, or lower levels of cortical htsN4 protein, or both, contribute to the effect. In addition, most extant *hts* mutations are zygotic lethal, and it is not certain that mutations that specifically affect the N4 variant currently exist. A second prediction is that expression of an artificial, non-localizable *htsN4* mRNA and protein may reproduce some or all aspects of the cytoskeletal phenotype in a *swallow*$^+$ background. Both of these approaches are in progress.

The observations reported here are not in conflict with other studies that show that microtubule integrity is required for the maintenance of *bicoid/htsN4* mRNA localization (Pokrywka and Stephenson 1991; Pokrywka et al. 2000), or with a study that demonstrates the association of swa protein and the 8 kDa dynein light chain protein (Schnorrer et al. 2000). Schnorrer et al. proposed that swa protein serves as a link between a *bicoid/htsN4* mRNA-containing particle and the dynein complex, which is in turn associated with the microtubule cytoskeleton. Since htsN4 probably acts as an actin cytoskeletal regulatory protein, the simplest hypothesis that combines all of the available data is that swa functions only in RNA localization, mediating the association between mRNA molecules and the microtubule cytoskeleton, and that actin cytoskeletal defects in *swallow* mutants are due to the failure to localize *htsN4* mRNA and protein.

Acknowledgements This research was supported by grant IBN9630705 from the National Science Foundation. J. Meng was partially supported by Graduate Council Fellowships from the Graduate School of the University of Alabama. We thank Dr. Nancy Pokrywka for comments on the manuscript, and Jola Nunley for assistance with confocal microscopy.

References

Baker J, Theurkauf WE, Schubiger G (1993) Dynamic changes in microtubule configuration correlate with nuclear migration in the preblastoderm *Drosophila* embryo. J Cell Biol 122:113–121

Bashirullah A, Cooperstock RL, Lipshitz HD (1998) RNA localization in development. Annu Rev Biochem 67:335–394

Berleth T, Burri M, Thoma G, Bopp D, Richstein S, Frigerio G, Noll M, Nüsslein-Volhard C (1988) The role of localization of *bicoid* RNA in organizing the anterior pattern of the *Drosophila* embryo. EMBO J 7:1749–1756

Chao YC, Donahue KM, Pokrywka NJ, Stephenson EC (1991) Sequence of *swallow*, a gene required for the localization of *bicoid* message in *Drosophila* eggs. Dev Genet 12:333–341

Dassow G von, Schubiger G (1994) How an actin network might cause fountain streaming and nuclear migration in the syncytial *Drosophila* embryo. J Cell Biol 127:1637–1653

Ding D, Parkhurst SM, Lipshitz HD (1993) Different genetic requirements for anterior RNA localization revealed by the distribution of Adducin-like transcripts during *Drosophila* oogenesis. Proc Natl Acad Sci USA 90:2512–2516

Driever W, Nüsslein-Volhard C (1988) The bicoid protein determines position in the *Drosophila* embryo in a concentration-dependent manner. Cell 54:95–104

Edwards KA, Demsky M, Montague RA, Weymouth N, Kiehart DP (1997) GFP-moesin illuminates actin cytoskeleton dynamics in living tissue and demonstrates cell shape changes during morphogenesis in *Drosophila*. Dev Biol 191:103–117

Ferrandon D, Elphick L, Nüsslein-Volhard C, St Johnston D (1994) Staufen protein associates with the 3′UTR of *bicoid* mRNA to form particles that move in a microtubule-dependent manner. Cell 79:1221–1232

Ferrandon D, Koch I, Westhof E, Nüsslein-Volhard C (1997) RNA-RNA interaction is required for the formation of specific *bicoid* mRNA 3′ UTR-STAUFEN ribonucleoprotein particles. EMBO J 16:1751–1758

Frohnhöfer HG, Nüsslein-Volhard C (1987) Maternal genes required for the anterior localization of *bicoid* activity in the embryo of *Drosophila*. Genes Dev 1:880–890

Gardner K, Bennett V (1987) Modulation of spectrin-actin assembly by erythrocyte adducin. Nature 328:359–362

Hatanaka K, Okada M (1991) Retarded nuclear migration in *Drosophila* embryos with aberrant F-actin reorganization caused by maternal mutations and by cytochalasin treatment. Development 111:909–920

Hegde J, Stephenson EC (1993) Distribution of swallow protein in egg chambers and embryos of *Drosophila melanogaster*. Development 119:457–470

Huang Z, Pokrywka NJ, Yoder JH, Stephenson EC (2000) Analysis of a *swallow* homologue from *Drosophila pseudoobscura*. Dev Genes Evol 210:157–161

Hughes CA, Bennett V (1995) Adducin: a physical model with implications for function in assembly of spectrin-actin complexes. J Biol Chem 270:18990–18996

Karr TL, Alberts BM (1986) Organization of the cytoskeleton in early *Drosophila* embryos. J Cell Biol 102:1494–1509

Kuhlman PA, Hughes CA, Bennett V, Fowler VM (1996) A new function for adducin. Calcium/calmodulin-regulated capping of the barbed ends of actin filaments. J Biol Chem 271:7986–7991

Li X, Matsuoka Y, Bennett V (1998) Adducin preferentially recruits spectrin to the fast growing ends of actin filaments in a complex requiring the MARCKS-related domain and a newly defined oligomerization domain. J Biol Chem 273:19329–19338

Lin H, Yue L, Spradling AC (1994) The *Drosophila* fusome, a germline-specific organelle, contains membrane skeletal proteins and functions in cyst formation. Development 120:947–956

Matsuoka Y, Li X, Bennett V (1998) Adducin is an in vivo substrate for protein kinase C: phosphorylation in the MARCKS-related domain inhibits activity in promoting spectrin-actin complexes and occurs in many cells, including dendritic spines of neurons. J Cell Biol 142:485–497

Mermall V, Miller KG (1995) The 95F unconventional myosin is required for proper organization of the *Drosophila* syncytial blastoderm. J Cell Biol 129:1575–1588

Pokrywka NJ, Stephenson EC (1991) Microtubules mediate the localization of *bicoid* RNA during *Drosophila* oogenesis. Development 113:55–66

Pokrywka NJ, Fishbein L, Frederick J (2000) New phenotypes associated with the *swallow* gene of *Drosophila*: evidence for a general role in oocyte cytoskeletal organization. Dev Genes Evol 210:426–435

Postner MA, Miller KG, Wieschaus EF (1992) Maternal effect mutations of the *sponge* locus affect actin cytoskeletal rearrangements in *Drosophila melanogaster* embryos. J Cell Biol 119:1205–1218

Raff JW, Glover DM (1988) Nuclear and cytoplasmic mitotic cycles continue in *Drosophila* embryos in which DNA synthesis is inhibited with aphidicolin. J Cell Biol 107:2009–2019

Schnorrer F, Bohmann K, Nüsslein-Volhard C (2000) The molecular motor dynein is involved in targeting Swallow and *bicoid* RNA to the anterior pole of *Drosophila* oocytes. Nat Cell Biol 2:185–190

Stephenson EC, Mahowald AP (1987) Isolation of *Drosophila* clones encoding maternally restricted RNAs. Dev Biol 124: 1–8

St Johnston D, Brown NH, Gall JG, Jantsch M (1992) A conserved double-stranded RNA-binding domain. Proc Natl Acad Sci USA 89:10979–10983

Sullivan W, Theurkauf WE (1995) The cytoskeleton and morphogenesis of the early *Drosophila* embryo. Curr Opin Cell Biol 7:18–22

Sullivan W, Minden JS, Alberts BM (1990) *daughterless-abo-like*, a *Drosophila* maternal-effect mutation that exhibits abnormal centrosome separation during the late blastoderm divisions. Development 110:311–323

Sullivan W, Fogarty P, Theurkauf W (1993) Mutations affecting the cytoskeletal organization of syncytial *Drosophila* embryos. Development 118:1245–1254

Theurkauf WE, Smiley S, Wong ML, Alberts BM (1992) Reorganization of the cytoskeleton during *Drosophila* oogenesis: implications for axis specification and intercellular transport. Development 115:923–936

Wang S, Hazelrigg T (1994) Implications for *bcd* mRNA localization from spatial distribution of exu protein in *Drosophila* oogenesis. Nature 369:400–403

Whittaker KL, Ding D, Fisher WW, Lipshitz HD (1999) Different 3′ untranslated regions target alternatively processed *hu-li tai shao* (*hts*) transcripts to distinct cytoplasmic locations during *Drosophila* oogenesis. J Cell Sci 112:3385–3398

Wilhelm JE, Mansfield J, Hom-Booher N, Wang S, Turck CW, Hazelrigg T, Vale RD (2000) Isolation of a ribonucleoprotein complex involved in mRNA localization in *Drosophila* oocytes. J Cell Biol 148:427–440

Yasuda GK, Baker J, Schubiger G (1991) Independent roles of centrosomes and DNA in organizing the *Drosophila* cytoskeleton. Development 111:379–391

Yue L, Spradling AC (1992) *hu-li tai shao*, a gene required for ring canal formation during *Drosophila* oogenesis, encodes a homolog of adducin. Genes Dev 6:2443–2454

Zaccai M, Lipshitz HD (1996) Role of *Adducin-like* (*hu-li tai shao*) mRNA and protein localization in regulating cytoskeletal structure and function during *Drosophila* oogenesis and early embryogenesis. Dev Genet 19:249–257

Zalokar M, Audit C, Erk I (1975) Developmental defects of female-sterile mutants of *Drosophila melanogaster*. Dev Biol 47:419–432